LC-DET-2001-029
20 February, 2001

Performance study of the proposed TESLA detector using a realistic track reconstruction package

T. Behnke[1], G.A. Blair[2], I. Božović-Jelisavčić[3], M. Elsing[4], K. Harder[1], R. Hawkings[4], K. Mönig[3], H. Vogt[3], D. Wicke[4]

[1] *DESY, D-22603 Hamburg*
[2] *Royal Holloway and Bedford New College, University of London, UK*
[3] *DESY, D-15735 Zeuthen*
[4] *EP Division, CERN, CH-1211 Geneva 23, Switzerland*

Abstract

In this note results of a performance study of the tracking system of the proposed TESLA detector are presented based on a realistic track reconstruction package. The code used was developed from existing FORTRAN and C packages from LEP experiments, which were modified to match the different detector specifications and background levels of a next generation linear collider detector. In the article performance issues of the charged track reconstruction system as well as detector resolution aspects are addressed. The track reconstruction operates on a detailed GEANT-based simulation of the TESLA detector proposal, including full simulation of the expected beam-related background in all subdetectors.

1 Introduction

The enormous physics program [1] for an experiment at a e^+e^- linear collider sets the challenges for the detector design. Performance goals for the tracker are excellent vertex resolution for heavy quark and τ identification, together with an accurate momentum determination, high redundancy to ensure good jet-jet reconstruction and good hermeticity in the forward direction. Vertex reconstruction will be needed to study new physics which involves heavy flavours, like Higgs and top decays. The higher energy at a linear collider compared to LEP will produce more energetic and therefore narrower jets. Redundant information in a many-layered tracker will be mandatory to resolve high energy jets into several particles. Many of the top, W^+W^- and SUSY channels are

characterised by missing energy signatures, which will need a hermetic detector to identify these events.

As a result of the present DESY/ECFA study, a baseline tracker design with two options for the vertex detector is proposed [2]. The specifications of both variants are implemented into the simulation package BRAHMS [3]. The subject of this article is to document the performance of both designs and to ensure that both meet the physics requirements. A complete pattern recognition package to reconstruct charged tracks was developed based on existing LEP software in order to obtain realistic results from the simulation data. This allows to study reconstruction efficiencies and rates of fake reconstructed tracks, as well as vertexing and momentum resolutions. At the same time effects of machine backgrounds and double track resolutions are taken into account. For the study the solenoid magnetic field is assumed to be 3 Tesla. The proposed coil for the TESLA detector is designed for a 4 Tesla field, but one intention of this note is to prove that track reconstruction with sufficient quality will also work in a more difficult environment than foreseen in the design. Therefore several system parameters were chosen with safety margins.

After a short overview over the two alternative detector layouts under discussion, a more detailed description of the reconstruction package is given to illustrate the level of detail included in the study. The results of the performance study are then discussed in view of the performance goals outlined above.

2 The detector layout

In this section a short overview over the tracker design is given. The two design variants currently favoured in the present DESY/ECFA study differ in the choice of the central vertex detector technology. Either Charged Coupled Devices (CCD) or hybrid Active Pixel Sensors (APS) could provide the performance required for the vertex detector. Additional technological options like CMOS pixel detectors are being developed [4], but have not yet led to a full mechanical design. In the following, both the CCD and the APS design are briefly discussed. More information can be found in Ref. [2].

A schematic view of the proposed TESLA detector [2] is shown in Figure 1. In the central region (see Figure 2) the innermost detector is a five layer CCD pixel detector (VTX), followed by two layers of double sided silicon strip detectors (SIT) and the TPC as the principal tracking detector. The forward direction is covered by 7 additional discs (FTD), 3 pixel layers and 4 layers of double sided silicon detectors. The momentum resolution of muons in the forward region is improved by a forward tracking chamber (FCH) behind

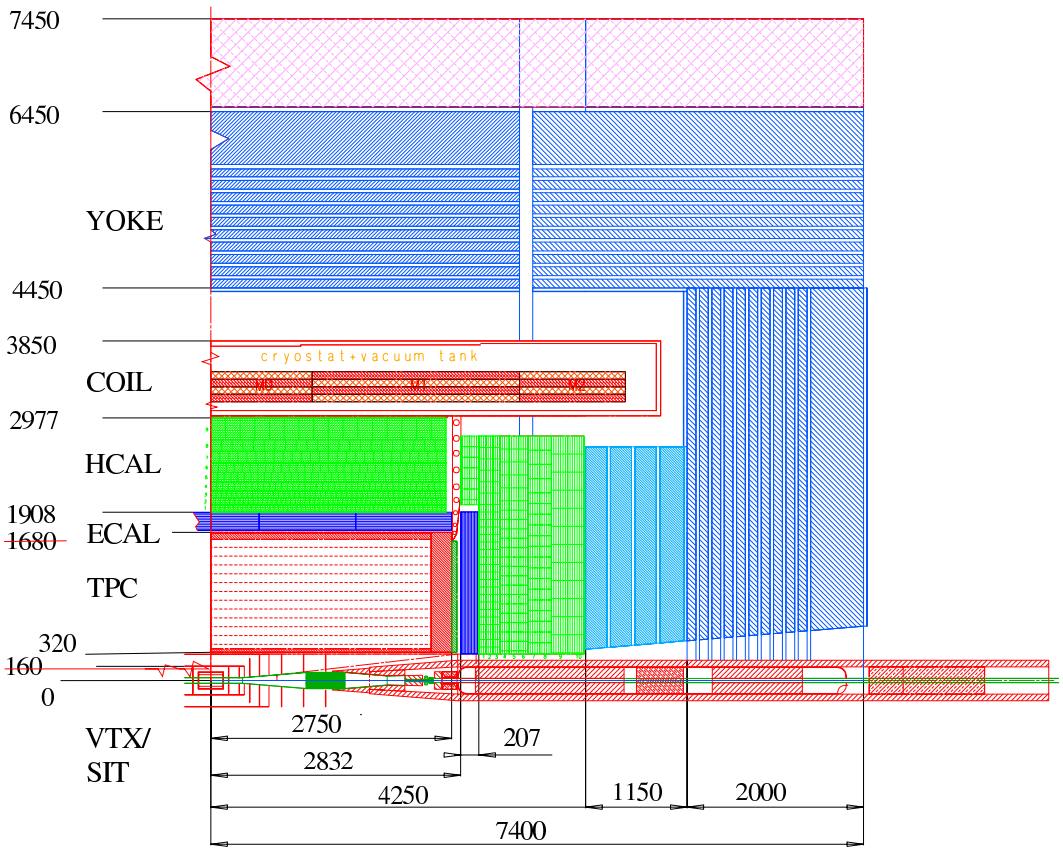

Fig. 1. A schematic view of one quadrant of the proposed TESLA detector. All dimensions are in mm. This Figure is taken from Ref. [2].

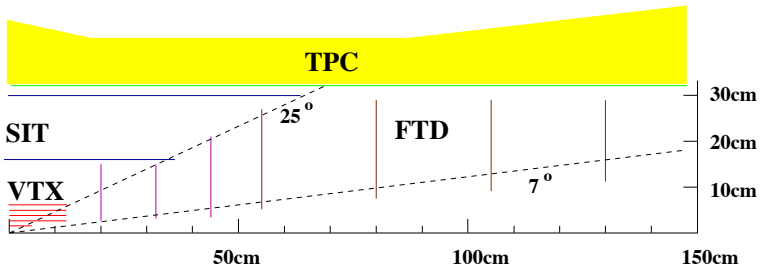

Fig. 2. Detailed view of the inner detector part as foreseen in the CCD option. This Figure is taken from Ref. [2].

the TPC endcaps. The FCH is supposed to consist of 12 layers of straw tubes in three different orientations.

Figure 3 shows the alternative design option for the central detector system, where the five layer CCD device is replaced by three layers of active pixel detectors (APS) with a conical detector endcap on the outermost layer. This

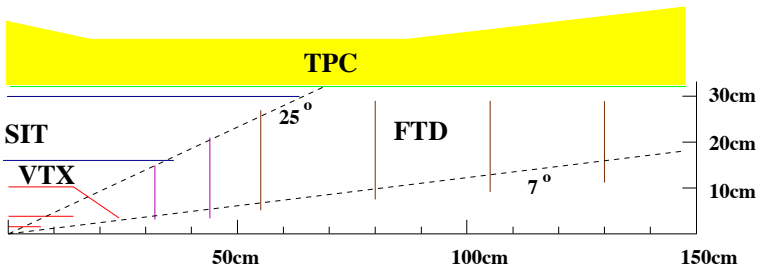

Fig. 3. Detailed view of the inner detector part as foreseen in the APS option. In comparison to the CCD variant, 3 vertex detector layers and one conical endcap are used instead of the five layer CCD device, and the innermost FTD layer as present in the CCD option is not foreseen in the APS design.

goes along with a modification of the FTD system in the sense that the innermost disk foreseen for the CCD option will not be used in the APS design. The coverage of the different detector components is summarised in Table 1.

2.1 Detector specifications

A TPC is foreseen as large tracking device for the linear collider detector, with a single hit design resolution varying between 50μm and 200μm in the $r\phi$ plane, depending on the drift distance [5]. The simulation software uses a constant $r\phi$ resolution of 160μm as approximation. A resolution of 1mm is expected along the z direction. A TPC combines several advantages: The number of pad rows and thus the redundancy for track reconstruction can be very large. The TESLA detector TPC is assumed to have 200 pad rows, allowing easy kink-finding and reconstruction of neutral particle decay vertices far from the interaction region. Resolution degradation due to multiple scattering is minimised, because the TPC gas is rather thin, and in the barrel region there is no additional material than the inner field cage. Furthermore particle identification is easily performed with dE/dx measurements. The number of pad rows has been optimized for momentum and dE/dx resolution [5,6]. Disadvantages of a TPC clearly are rather thick endcaps and a limited capability to resolve very close tracks. Conservative values of 3.3mm in $r\phi$ and 14mm in z are assumed as double hit resolution.

Major task of a Silicon microvertex detector is the precise measurement of impact parameters in order to allow efficient vertex reconstruction. The high density of tracks in narrow jets close to the interaction region increases the demands imposed on a vertex detector. A pixel device with a point resolution of not more than several micrometer is therefore mandatory for a linear collider detector. Three alternative designs are under study. The highest possible res-

detector	radial coverage [cm]	z coverage [cm]	$\|cos(\Theta)\|$ range	comment
VTX (CCD)	1.55	-5.0..+5.0	0..0.955	
	2.4	-12.5..+12.5	0..0.982	
	3.6	-12.5..+12.5	0..0.961	
	4.8	-12.5..+12.5	0..0.934	
	6.0	-12.5..+12.5	0..0.902	
VTX (APS)	1.55	-7.30..+7.30	0..0.978	
	3.75	-14.3..+14.3	0..0.967	
	10.0	-14.3..+14.3	0..0.820	coverage without endcap
		-24.3..+24.3	0..0.990	including conical endcap
FTD	2.8..15.0	±20.0	0.800..0.990	CCD option only
	3.3..15.0	±32.0	0.906..0.995	
	4.3..22.0	±44.0	0.894..0.995	
	5.3..28.0	±55.0	0.891..0.995	
	7.4..30.0	±80.0	0.936..0.996	
	9.4..30.0	±105	0.962..0.996	
	11.5..30.0	±130	0.974..0.996	
SIT	16.0	-38.0..+38.0	0..0.922	
	30.0	-66.0..+66.0	0..0.910	
TPC	38.6..162.6	-250..+250	0..0.988	200 pad rows
FCH	32.0..160	±273..±279	0.863..0.994	12 layers

Table 1
Subdetector coverage for the proposed TESLA detector for APS and CCD vertex detector options.

olution and very thin detector layers are expected to be achievable with either CCD or CMOS detector systems. Detailed studies are especially available for CCD devices and show that a detector with 3.5 micron point resolution and 0.06% radiation length thickness per layer is feasible [7]. This would allow to operate a five layer CCD detector in a cryostat with still very good material budget.

A CCD detector is read out by shifting the information stored in the individual pixels cell by cell along readout columns. In the TESLA bunch structure environment, the physics and background hits of 60 bunch crossings are therefore

accumulated until the signal enters the front-end electronics. A pattern recognition algorithm for a CCD vertex detector will thus have to deal with a much larger number of background hits than that for a detector with immediate readout of every individual pixel.

Another proposal for a vertex detector for the TESLA linear collider uses hybrid active pixel sensors (APS), which feature readout drivers integrated into the active detector material. This provides simpler and faster readout capabilities, but at the cost of larger pixels and thicker detector layers. At the current level of technological development it is expected that three APS layers are the optimal compromise between material and tracking performance. A point resolution of 7μm is envisioned. Full GEANT simulation is available in the BRAHMS software package for CCD and APS option.

Neither TPC nor vertex detector provide sufficient coverage to perform track reconstruction with good momentum resolution in the angular region very close to the beam pipe. Therefore dedicated Silicon disk-shaped detectors are proposed to achieve a maximal degree of hermeticity with the tracking detectors. Three Silicon disks within less than 50 cm on both sides of the interaction region provide pixels with roughly $50\mu\text{m}\times15\mu\text{m}$ resolution to complement the CCD vertex detector. The innermost pair of disks is replaced by conical detector endcaps attached to the outer vertex detector layer in the APS design. Farther away than 50 cm from the collision region double sided strip detectors can easily cope with the remaining background and track density; four disks of 25μm effective point resolution are assumed at z coordinates of $\pm$55cm to $\pm$130cm. A strip detector has been simulated in a worst case scenario with strips running exactly in the r and $r\phi$ direction, and no significant degradation of the performance has been seen. This simulation has however not yet been included in the study presented here.

TPC, vertex detector and forward tracker comprise the main track detectors of the proposed linear collider detector. Special emphasis lies on the fact that these subdetectors are capable of independent track reconstruction, with restrictions in the case of the APS vertex detector. These stand-alone capabilities are considered advantageous for internal alignment of the silicon detectors, and for the redundancy of the track reconstruction in general. Further detector systems are added, though, to improve the overall performance in specific tasks.

Two layers of high resolution double-sided silicon strip detectors, the Silicon Intermediate Tracker (SIT), are foreseen to bridge the gap between vertex detector and TPC inner radius. With a per-layer hit resolution of 10μm in $r\phi$, and 50μm in z, the outer layer at its radius of 30 cm and thus large lever-arm with respect to the precise vertex detector layers plays an important role in achieving the global momentum resolution designed to be $\delta(\frac{1}{p_t}) \leq 5\times10^{-5}(\text{GeV/c})^{-1}$.

The inner layer at 16 cm radius has been added to the proposal to improve reconstruction of vertices from long-lived strange particles in the otherwise uncovered radial range of 6 (CCD) or 10 (APS) cm and 31 cm, the inner edge of the TPC field cage. The APS vertex detector furthermore relies on the additional silicon layers to ensure the possibility of performing pattern recognition independently from the TPC. No simulation of silicon strip detectors is currently implemented in the simulation. However, the hit densities on the SIT layers are comparably low, and thus no noticeable effect on the track reconstruction performance is expected from the imprecise modeling of this detector. This is especially true since the availability of full 3d information both inside (VTX) and outside (TPC) the SIT will allow very good discrimination between true and mirror hits.

The full system of silicon based high precision detectors is designed to ensure a coverage of at least five space points throughout the whole angular reach of the tracking devices. In addition to the stand-alone pattern recognition capabilities of vertex detector and forward tracker, this provides a good basis for a combined silicon detector pattern recognition, which is advantageous in the overlap region between vertex detector and forward tracker.

Tracks passing through the TPC endcaps do in general not traverse all TPC pad rows. Smaller number of hits for use by a track fit and the shorter track length in the TPC at decreasing polar angle degrade the momentum resolution achievable for these tracks. Additional Forward Chambers (FCH) are proposed behind the TPC endcaps to recover from this degradation at least for muons. Other particles are expected to be scattered significantly in the approximate 30% of a radiation length material in the endcaps. Twelve layers of straw tubes in three different orientations are the technology of choice for the FCH, which allows internal pattern recognition. A resolution of 100μm is foreseen, and a double hit resolution of the same size has been assumed.

Table 2 gives an overview of the detector specifications as implemented in the full detector simulation. The simulation matches the detector proposal in Ref. [2], with the exception of the few details mentioned above.

2.2 Background levels in the different subdetectors

Sources of background are beam-beam effects, synchrotron radiation and debris from the final quadrupol, as well as muon background from upstream sources [2]. For the purpose of this study the effects due to e^+e^- pair production are dominant, and their effects are incorporated in the simulation package.

Table 3 gives an overview of the expected amount of background hits per

subdetector	resolution	space points
VTX (CCD)	3.5μm	5
VTX (APS)	7μm	3
pixel FTD	15μm$\times 50\mu$m	2, 3 (APS, CCD)
strip FTD	25μm	4
SIT	10μm$\times 50\mu$m	2
TPC	160μm ($r\phi$), 1 mm (z)	200
FCH	100μm	12 strips

Table 2
Subdetector specifications for the proposed TESLA detector as present in the simulation software [3]. The simulation matches the technical proposal, with the exception of SIT and outer FTD detectors. These are proposed as double strip detectors, whereas the simulation contains pixel readout. The assumption of a constant TPC $r\phi$ resolution is an approximation of a linear dependence observed in TPC drift studies [5].

bunch crossing in each tracking detector [2]. A conservative estimate of 1% total background occupancy has been assumed for the TPC. It is assumed that all other subdetectors except the CCD vertex detector option can be read out once per bunch crossing; thus, the numbers given in Table 3 reflect directly the amount of background present in the reconstruction chain. The CCD vertex detector accumulates background over 60 bunch crossings before the event data enter the reconstruction [7]; therefore each event in the CCD is overlaid by 60 times the number of background hits given in the table.

3 The full reconstruction package

The track reconstruction system that has been implemented in the BRAHMS detector simulation software package is designed modularly. A global steering package collects hits from all tracking subdetectors in a common bank structure. These hits are then passed over to pattern recognition packages that perform a local track search in the respective subdetector, or combination of subdetectors. Currently three pattern recognition packages are in use: A dedicated TPC pattern recognition is optimised to cope with specific TPC properties like limited double-track resolution and a large number of space points. A full Silicon pattern recognition exploits the homogeneous design of the inner tracking to combine the information delivered by vertex detector, forward tracker and SIT for performing a track search. A Forward Chamber pattern recognition package is specifically designed for wire chamber signal processing.

subdetector	hits per bunch crossing			
	500 GeV		800 GeV	
	3 T	4 T	3 T	4 T
CCD layer 1	548	350	616	422
CCD layer 2	224	132	264	119
CCD layer 3	76	42	80	57
CCD layer 4	72	26	31	23
CCD layer 5	26	17	23	11
APS layer 1	800	511	899	616
APS layer 2	87	48	92	65
APS layer 3	21	15	18	10
APS cone	71	34	84	54
FTD layer 1	71	34	84	54
FTD layer 2	58	33	68	35
FTD layer 3	38	24	37	26
FTD layer 4	24	16	27	26
FTD layer 5	26	16	32	16
FTD layer 6	22	13	16	14
FTD layer 7	12	12	11	11
SIT layer 1	22	23	16	17
SIT layer 2	15	7	9	5
FCH, per layer	19	10	9	11
TPC (tracks)	7	5	7	8

Table 3
Number of background hits per bunch crossing originating from e^+e^- pair production in all detector systems [2]. FTD and FCH rates are summed over both sides. The amount of background entering the reconstruction has to be multiplied by 60 for the CCD vertex detector layers, because the CCD readout takes the time equivalence of 60 bunch crossings [7].

The track candidates found by the local pattern recognition are passed back to the steering routine, which converts track candidates from the local pattern recognition routines into a common data format to be used by the global track search. All hits found in the silicon detectors are also passed on to the global track search separately. This is done to be able to improve the local silicon pattern recognition in a second step, including additional information from

the TPC and FCH.

A high efficiency is maintained by performing the global track search without taking care of ambiguities. Any sensible combination of hits and local tracks is selected if certain minimal quality criteria are fulfilled, and track candidate sharing one or more hits are not excluded at this stage. The resolving of these ambiguities is done in a final step, where all track candidates found in the event are treated at once to optimise the overall fit result.

The structure of the track search implemented in the BRAHMS linear collider detector simulation software has been adapted from the DELPHI experiment at LEP, where this strategy has proven itself highly successful. An overview of the structure of the track reconstruction system in BRAHMS is given in Figure 4.

3.1 The global steering

The execution of the reconstruction package is controlled by a global steering. It serves as the interface to the simulation package for receiving the information. Necessary conversions between different ways of parameterising hits and helices are done. The simulation data, intermediate results and the reconstructed event are stored in an event data space (ZEBRA) which allows to cope with the huge memory requirements due to simulated backgrounds. The global steering calls the different reconstruction processors which are discussed in the following.

3.2 The local reconstruction packages

The first layer of pattern recognition involves a local pattern recognition for the different subdetectors. First all hits in the subdetectors are converted into space points used in the later reconstruction. Three subsystems have a detailed local pattern recognition to exploit the stand-alone tracking capability of the devices. The first is the full system of silicon tracking detectors, comprising the CCD or APS detector, the SIT and the FTD. Another detector having a local pattern recognition is of course the TPC. A third local track search deals with the information obtained from the forward chambers. The task of those local reconstruction codes is to find short local track elements which will be used in the later processing as seeds for the final track searches.

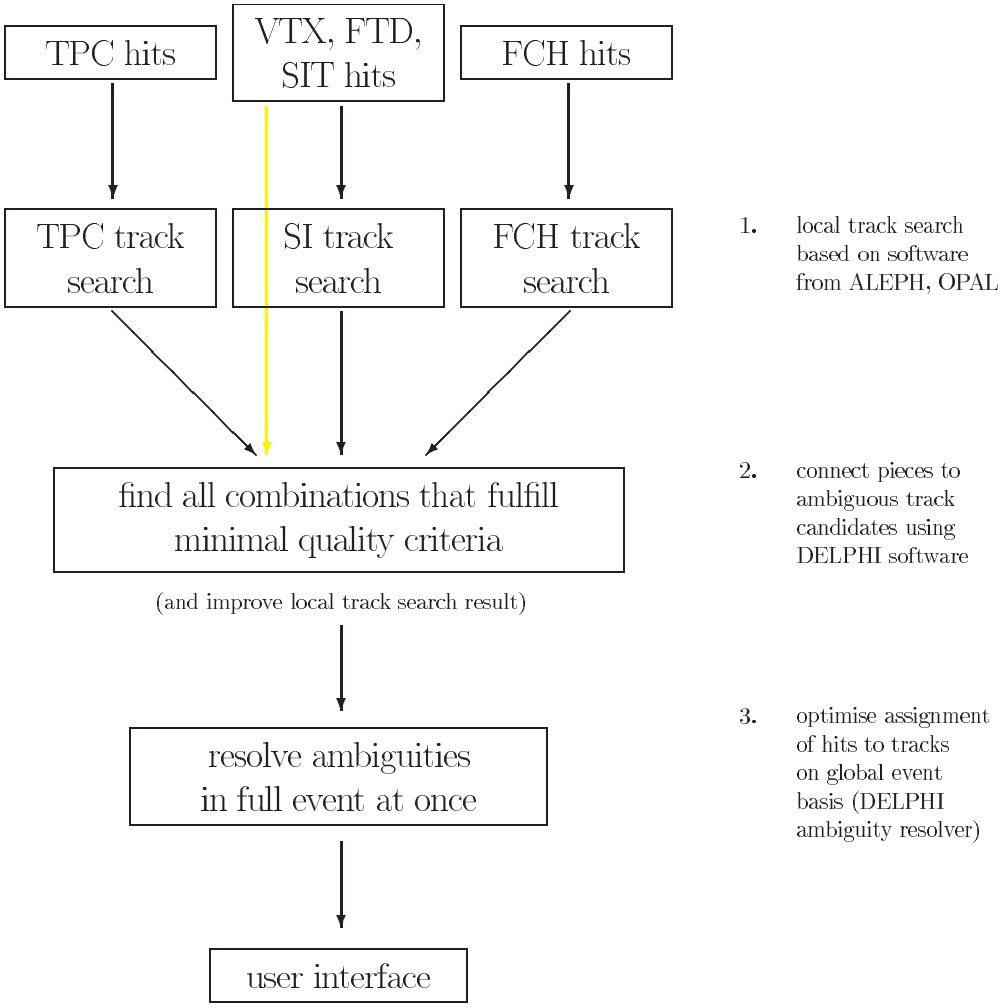

Fig. 4. A schematic view of the track reconstruction system. The three main stages of data processing are explained in the text. Each box corresponds to a separate software module. Additional packages that are not represented in this overview are the track fit module, and the global steering that controls data flow between and storage for all packages.

3.2.1 The pattern recognition for the silicon trackers

The silicon trackers feature cylindrical layers of pixel detectors (CCD or APS vertex detector), cylindrical layers of double-sided strip detectors (SIT), silicon pixel detector disks (inner FTD), and double-sided strip detector disks (outer FTD). The APS design also includes conical pixel detector endcaps. Combining all these different detector types in such a way that a common pattern recognition program can treat them simultaneously is clearly a non-trivial task. Although the strip detector simulation for SIT and outer FTD is not yet used in this study, a structure to cope with these detector types has already been included in the track search. This approach starts with trans-

forming the strip detector readout into pseudo-pixels. All positions where a front side strip with a signal crosses a back side strip with a signal are assumed to be separate hits, although in general different assumptions on where the actual hits took place are mutually exclusive. Solutions that are mutually excluded are marked as such (see Section 3.5), but these exclusions are ignored until later in the track reconstruction process, where information from other subdetectors is included to help decide which solution is most likely correct. This way the number of hits that has to be taken care of by the track search is generally much larger than in the case of true pixel detectors, but on the other hand the track search can be performed with a very simple algorithm that only has to be able to cope with 3d pixels.

Once all (pseudo- and real) pixels are made available, the track search starts with all combinations of hits from the outermost three layers with hits in a number of angular subdivisions of the silicon detectors. A helix fit is attempted for each such combination, and if the fit succeeds with acceptable χ^2, matching hits on the next inner layer are added to the candidate. All layers with matching hits are thus successively being scanned for hits to be added to the track candidates. Chains that are found in neighbouring angular subdivisions are finally merged together if they match. A detailed description of the algorithm can be found in Ref. [8].

It has to be pointed out that two or more local track candidates in the silicon detectors may share one or more hits. Although these candidates are in fact mutually exclusive, none of these is rejected. Even candidates that do not share hits may be excluded against each other if they contain pseudo-hits from double-sided strip layers that are mutually exclusive, as indicated above. Candidates of either type are marked as being excluded against each other, but they are kept for further analysis. The decision which candidate is most likely correct is not taken before the information from other subdetectors can be taken into account, at a later stage in the track reconstruction.

The silicon vertex detector is the device that is closest to the interaction region. Therefore it suffers most from beam-related background (see Table 3). This is especially true for the CCD option, where background hits are accumulated over 60 bunch crossings. In this case, the track search has to deal with between 10^4 and 10^5 background hits overlaid over each physics event. It has been shown that this is feasible using the simple algorithm described above. An additional option, which has been used in this study, is to exclude the innermost one or two vertex detector layers from the initial local track search, and to collect hits on this layer only at a very late stage, where track candidates including information from all other detectors can be extrapolated towards the IP with maximal precision. Both options are foreseen in the track reconstruction software, but the latter has proven advantageous in terms of CPU time consumption, while the reconstruction performance is similar in

both cases.

3.2.2 TPC pattern recognition

The track search in the TPC is performed by a modification of the ALEPH TPC pattern recognition software. Hits in the TPC are sorted by radius and by ϕ coordinate. Chains of tracks are created by combining hits of the outermost pad rows, and then subsequently adding hits at smaller radii by a Kalman Filter algorithm, i.e. comparing the coordinates of hits in question with predicted coordinates calculated from a helix extrapolation of the current chain of hits. Deviations from a helix trajectory due to multiple scattering of particles in the TPC gas are taken into account.

Special care is taken to minimise disturbance by limited double hit resolution, which mainly affects the inner part of the TPC, where the distance of tracks in jets is frequently smaller than what can be resolved. TPC readout signals that are merged contributions from more than one actual hit are expected to have coordinates that are an average of the coordinates of the contributing hits. Including these hits into a track fit would therefore effectively degrade the resolution and decrease the efficiency of merging those track candidates with information from the silicon detectors. Merged hits can in principle be tagged by looking at the pulse height or shape. A different, purely geometrical approach is being followed in the software described here: The initial track search starting at the outermost pad row stops in the middle of the TPC sensitive radial range, safely outside the region where significant effects of limited double hit resolution are observed. The track candidates assembled in this initial search are then extrapolated into the inner radial region of the TPC volume, and regions are being searched for where at least two tracks come closer to each other than the expected double hit resolution. All hits in these regions are assumed to be distorted due to merging of several contributions, and are removed from the database. Only the remaining hits are then used in the second part of the local track search.

3.2.3 The forward chamber track search

Since the forward chambers are supposed to be constructed from twelve layers of straw tubes on each side of the detector, they do not provide space points, but only wire information. However, the chamber is designed to support full 3d track reconstruction following a principle already used at DELPHI. The twelve layers are grouped into six double-planes of parallel, but staggered wires. The wire orientation of each double plane is rotated by 60° with respect to the neighbouring double planes. This amounts to three different orientations in two sets of double-planes each.

Main task for the forward chambers is the reconstruction of high energy muons. The momentum resolution achieved by TPC and inner detectors alone degrades in the forward direction. Other particles than muons suffer from scattering in the TPC endcaps, and therefore the momentum resolution for these particles can hardly be improved by the FCH. As a consequence, the FCH track finding algorithm can be optimized for straight tracks originating from close to the IP without affecting the physics performance of the overall track reconstruction.

The first step is a search for hits on two near-by wires within each double plane. Only combinations that are compatible with a straight track coming from close to the IP are kept for further processing. For each hit both possible drift directions are taken into account. The second step is performed separately for the inner and outer set of three double-planes: From the hit combinations space points are reconstructed, where most of the fake combinations are rejected because of the redundant information in the three double planes. Pairs of such space-points from the inner and outer three double-planes are checked for being compatible with coming from a straight track originating in the IP. If they are, a full helix fit is performed using the information from all twelve planes.

3.3 The Kalman Filter track fit

A common track fit algorithm is applied to all local track candidates found by the subdetector pattern recognition packages, and to combinations of those (global track candidates). The track fit can operate on hits as well as full track parts. This is for example exploited in the final track fit, where the TPC contribution is not entered as single hits, but as a full set of track parameters as obtained from the local TPC track fit.

The track fit algorithm used is a Kalman Filter [9,10] which was developed for the DELPHI experiment. It is a fast recursive algorithm implemented using the weight matrix formalism. A Kalman Filter is an estimator for a linear system, while a track in a solenoid field is described by a helix. Therefore a Taylor expansion around a reference trajectory is used as a starting point to obtain a linear system. The fit is iterated to ensure good convergence.

The track fit takes into account the effects of multiple scattering and energy loss in the material. A simplified description of the detector material is sufficient for the purpose of track fitting. The geometry of the detailed detector material description of the TESLA detector simulation is approximated in the track fit by a sequence of surfaces, which are either cylinders around or planes perpendicular to the beam pipe. For each of these surfaces an apparent

thickness is specified in terms of radiation length and energy loss of a minimal ionising particle (for a particle crossing at 90°). Additional surfaces are introduced in the TPC drift volume to account for the dE/dx of particles in the drift gas.

In the track fit the effect of the multiple scattering is taken into account by increasing the error contour of the track extrapolation after crossing the material surface. The momentum dependent effect of the energy loss is taken into account by changing the curvature of the reference trajectory used for the Taylor expansion in the fit.

Another important feature of the fit is the logic to remove outliers. The fit is able to remove up to 3 measurements from a track candidate if it fails a fit χ^2 probability cut of 0.1%. This is a very effective filter to remove wrong associations of hits to tracks. A ranking of detectors to be removed is used in order not to remove the most precise measurement (e.g. the TPC track element) from the track. Called from the track search packages the fit always retains the track element which was used as a starting point to reconstruct the track.

3.4 The global track search

The task of the global track searches is to find all possible track candidates. A generic track search engine [11] is used to implement several track search strategies. For each of those strategies a two stage algorithm is executed. First, the track element used as a starting point are extrapolated to other detectors which do not yet contribute to the reconstruction. For each of those detectors a list of candidate hits or track elements within a road around the extrapolation is selected. Then a sorted loop over all candidate lists is done in order to find the longest possible track combinations. Here the Kalman Filter track fit is used as the major filter for rejecting fake combinations.

In the first stage of the processing an attempt is made to merge the track elements in the silicon tracker system with those in the TPC, which were both found by the local pattern recognitions. Starting from the silicon all matching TPC track elements are combined to track candidates and vice versa. Before each track candidate is fitted, the track elements in the silicon tracker system are replaced by the individual hits in the different layers. This allows to correctly take into account the multiple scattering and energy loss in the silicon tracker material by using the momentum estimate from the full track. Also, single fake hits can be removed from the track if the fit of the full track is rejected by the outlier logic of the Kalman Filter. Furthermore, the information that hits in the silicon are missing is used in the second stage of

the processing to improve the association efficiency.

After the first searches, the track candidates are extrapolated to all detectors (or silicon layers) which do not yet contribute to the reconstruction. This is done in steps. First, all candidates are extrapolated to the SIT layers and to the forward chambers and missing hits are added into the candidates. Then all FTD discs are scanned for additional hits. Missing hits in the VTX are added in three steps to allow for the background levels in the first layers. Hits in the outermost layers 3-5 (or layer 3 and the conical endcap in the APS option) are searched in a first step. For those candidates which already include VTX hits and have therefore very small extrapolation uncertainties, also the second layer is scanned for additional hits. Extrapolation onto the first vertex detector layer is performed in the final step.

At the end of this process all candidates found by the searches are stored in the event data space and sent to the ambiguity processor for resolving the left over ambiguities in the hit association to tracks.

3.5 The concept of "exclusions"

The result of track searches is a set of ambiguous track candidates with many possible associations of individual hits to different track candidates. Also the local pattern recognition of the different detectors can create ambiguous hit combinations. For example in the Silicon Intermediate Tracker space points are supposed to be reconstructed out of hits on the back-to-back module by combining the measurements in both orientations, as indicated above, so that hits from n tracks on a module lead to $n(n-1)$ mirror images. Such ambiguities need to be resolved in the process of the track reconstruction. It is beneficial to leave the decisions to the stage of the global event solution, since at this stage the full information of the reconstructed track candidates can be used to minimise mistakes.

All results from the different reconstruction packages are stored in the event data space. The structure allows for so called "logical exclusions" between objects like hits or track candidates. An "exclusion" signals that two objects use conflicting or common detector information and that for the final solution of the event such conflicts need to be resolved.

3.6 The event ambiguity processing

The ambiguity solution is a combinatorial problem. The task of the ambiguity processor is to decide about the association of hits and to select the best

tracks out of the set of mutually "excluded" candidates found by the search algorithms. The design of the ambiguity processor [12] was done in order to find a balance between performance and CPU consumption.

The ambiguity processor maximises a "score" function for a given event. The score of each track in the solution is determined by the number of hits associated to the track and the quality of the fit. A simple algorithm to resolve the event can start by selecting the track with the highest score. The hits associated to that track are removed from all other candidates. This implies refitting the candidates from which a hit has been dropped. The list of candidates is therefore changing in the course of the process. The process is iterated by selecting the next best track until no more candidates are left over. This algorithm is very fast, but any mistake at the beginning propagates through the rest of the event analysis. Another algorithm, which does not have this problem, would be to create all possible lists of tracks, which contain no "exclusions" anymore, in the same way as before. Here the list with the highest score would be selected. This algorithm is limited by combinatorics, because the number of lists increases very rapidly with the number of candidates.

The ambiguity processor is a mixture of both algorithms. It is a recursive algorithm, which in each step subdivides the event into sets of "excluded" tracks to resolve them independently. For each set all possible lists of tracks are tried. One track after the other is taken out of the set and each time the subset is resolved in the next recursion level. For each recursion the maximum possible score of the subset is calculated to truncate combinations below the current maximum. A fall back solution is implemented, which uses the simpler algorithm for a set in case it is not resolved after more than one second or the recursion depth is exceeding 9 levels.

Additional protections are needed. Sub-tracks created during the processing are rejected if they are only generated by splitting a long track. A list of bad tracks is used to reject detector combinations of poor quality or high risk of being fake.

The scoring function is tuned to optimise the track reconstruction efficiency and the hit association purity at the same time. For each track a score of 100 is assigned, while a detector measurement associated to the track is given a score between 1 and 20, depending on the quality of the measurement, and a logarithm of the χ^2 probability of the track fit is added to disfavour bad track candidates.

The result of the ambiguity processing is the final reconstruction result which is then stored in the event data space and used for analysis.

4 Performance of the proposed detector

Two reference event samples that represent different pessimistic scenarios are used for the evaluation of the linear collider detector tracking performance. Two-jet events created by $e^+e^- \to Z \to d\bar{d}$ reactions at 500 GeV centre-of-mass energy without initial state radiation comprise the main reference sample. These events contain high-multiplicity jets which are highly boosted and thus comparatively narrow. A second sample has mainly been chosen to push track reconstruction in the TPC to its limit by providing tracks that are extremely close to each other. $e^+e^- \to Z \to \tau^+\tau^-$ events at 800 GeV without initial state radiation, where each τ is forced to decay into three charged particles, have been selected for this task. Example events of both samples are shown in Figure 5.

Only tracks that fulfill certain quality cuts are being accounted for in the performance analysis. In order to avoid normalisation of the reconstruction efficiency to tracks which would not have been found even with ideal track reconstruction, all tracks are excluded that leave less than three hits anywhere in the detector. The hermetic detector design ensures that the fraction of tracks outside the beam pipe that cause less than three hits is practically zero. A minimal momentum of 1 GeV is required, and tracks that originate from secondary interactions with the detector material (e.g. conversion electrons) are rejected. The full angular extent of $|\cos(\theta)| < 0.995$ is evaluated. Both samples are processed with full background simulation in all subdetectors, including the equivalent of 60 bunch crossings of background in the CCD vertex detector.

4.1 Performance of the local pattern recognition packages

The result of the local track searches in the TPC, the silicon detectors and in the Forward Chambers are the starting point of the track reconstruction. Only tracks that are reconstructed in at least one of these three detector systems will show up in the sample of globally reconstructed tracks. The detector is designed to provide at least two independent systems capable of providing local track reconstruction over a maximal angular range. Thus a high level of redundancy is foreseen and evident in the performance figures presented in the following. Nevertheless, in order to achieve the full design performance of the detector as far as momentum and vertex resolution are concerned, maximal contribution of all available subdetectors to the reconstructed tracks is mandatory. Therefore, the local track search efficiency is a central figure of merit.

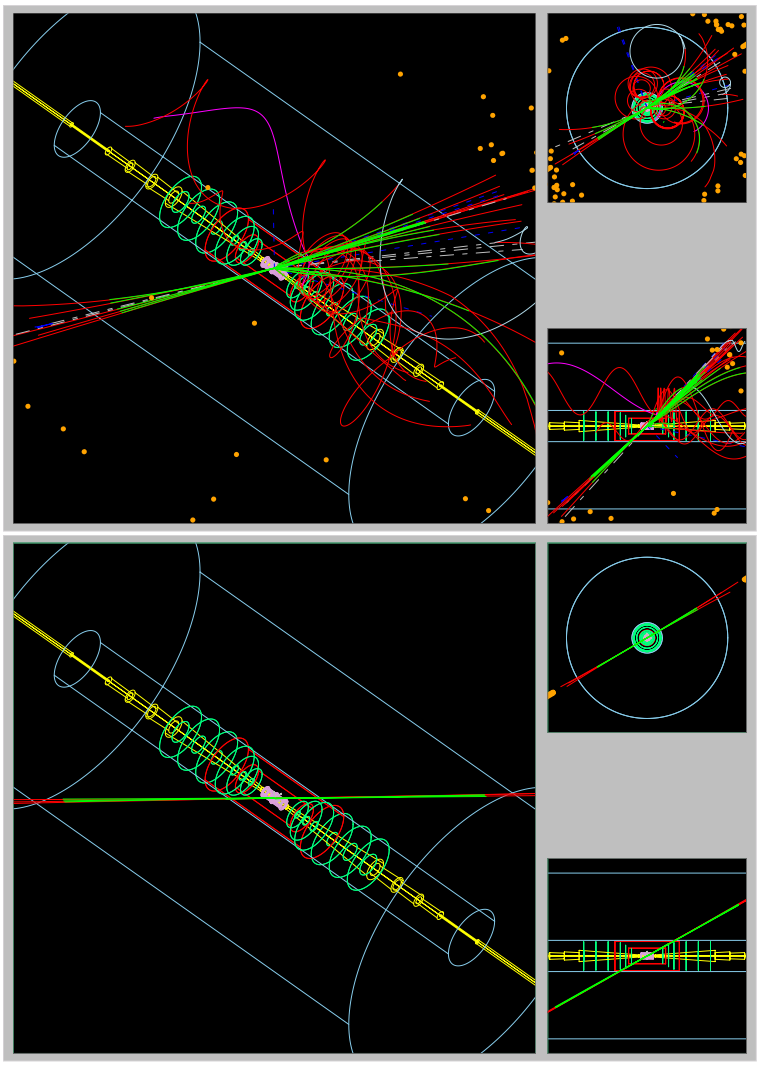

Fig. 5. BRAHMS event displays [13] of two reconstructed events after the complete processing. (top) A $Z \to d\bar{d}$ event at 500 GeV and (bottom) a $Z \to \tau^+\tau^-$ 3-prong event at 800 GeV. Charged tracks are shown in red, and the respective reconstructed tracks are overlaid in green.

The reconstruction of tracks in the TPC performs well as expected even for the narrow jets typical for $d\bar{d}$ events. A reconstruction efficiency of 98.1% despite a background occupancy of 1% has been found in this sample. As visible in Figure 6, mainly high momentum tracks contribute to the inefficiency. This is presumably due to jets with significantly less than the average multiplicity, where few high-momentum tracks traverse the TPC closer to each other than can be resolved given the limited double-hit resolution. This effect is much more prominent in the $\tau^+\tau^-$ reference sample (Figure 7), where almost all jets are of this type. As a consequence, the local reconstruction efficiency drops to just above 90% there. It will be shown later that this loss in efficiency is fully compensated by the redundant track searches in other subdetectors, mainly the silicon detectors. The fraction of fake tracks among the track candidates

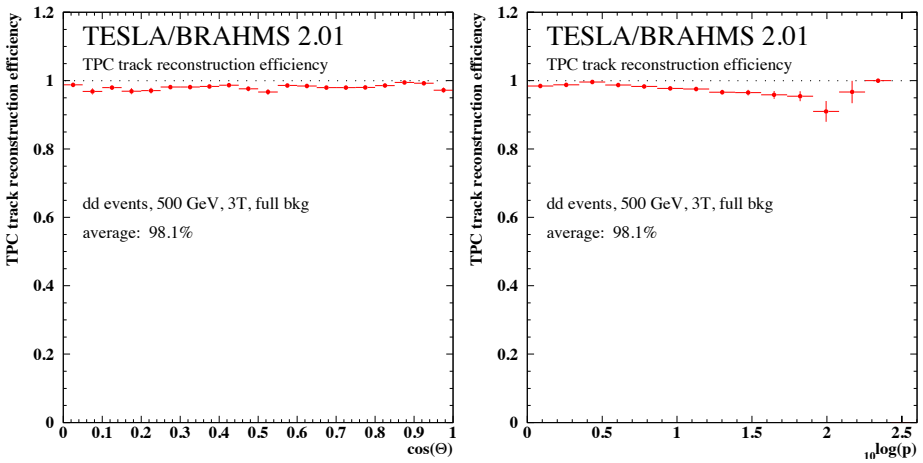

Fig. 6. Local track search efficiency in the TPC, with full background simulation on the $d\bar{d}$ reference sample, over $|\cos(\theta)|$ (left) and over the track momentum (right).

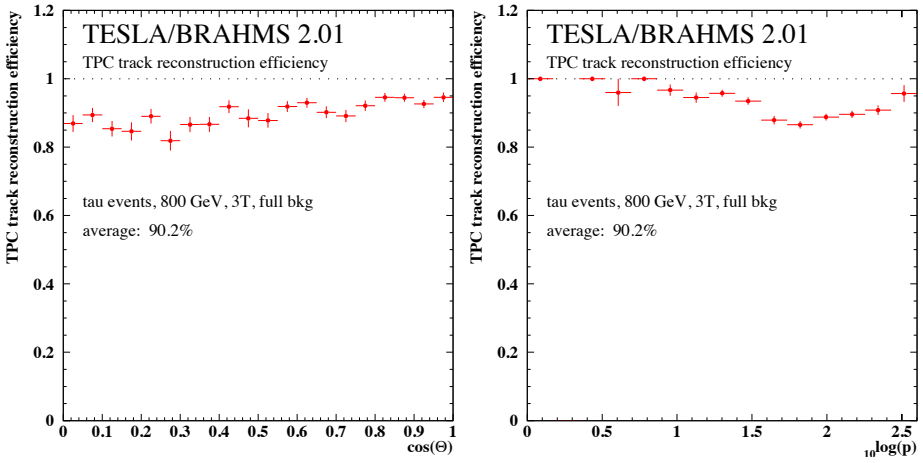

Fig. 7. Local track search efficiency in the TPC, with full background simulation on the $\tau^+\tau^-$ reference sample, over $|\cos(\theta)|$ (left) and over the track momentum (right).

is 0.4% for $d\bar{d}$ events, and raises to 2.1% in the $\tau^+\tau^-$ sample. A fraction of between 3% ($d\bar{d}$) and 8% ($\tau^+\tau^-$) of all tracks has been reconstructed in more than one piece, although no interaction other than multiple scattering took place during their traversal of the TPC. This effect is caused by hits that are merged with background hits or hits from close-by tracks. These hits appear shifted away from the track, or are removed by the hit-merging finder and interrupt the track search trying to follow tracks through the TPC. No attempts are currently made to merge this split tracks together in a later step of the track reconstruction, although this is foreseen in the reconstruction code.

The silicon detector track search has been investigated separately for CCD and APS option. The APS design achieves a reconstruction efficiency of 97.4% with full background, where mainly low-momentum tracks in the forward direction

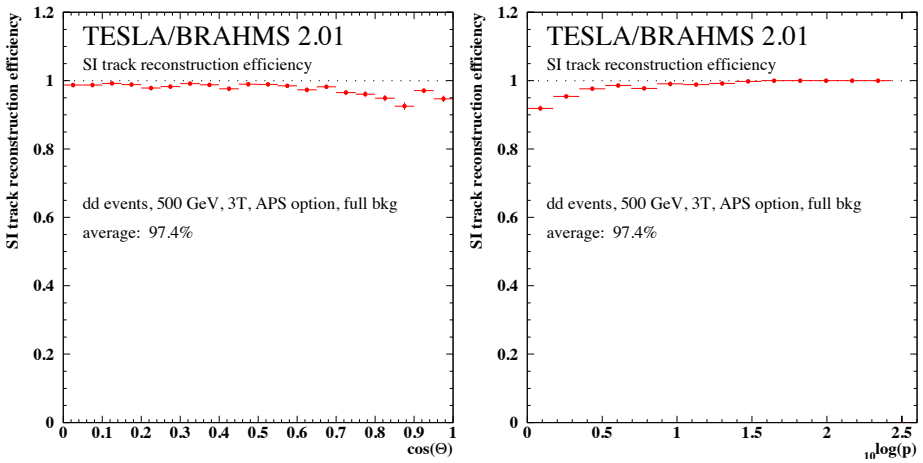

Fig. 8. Local track search efficiency in the APS variant of the central silicon detector system (APS-VTX, SIT, FTD), with full background simulation on the $d\bar{d}$ reference sample, over $|\cos(\theta)|$ (left) and over the track momentum (right).

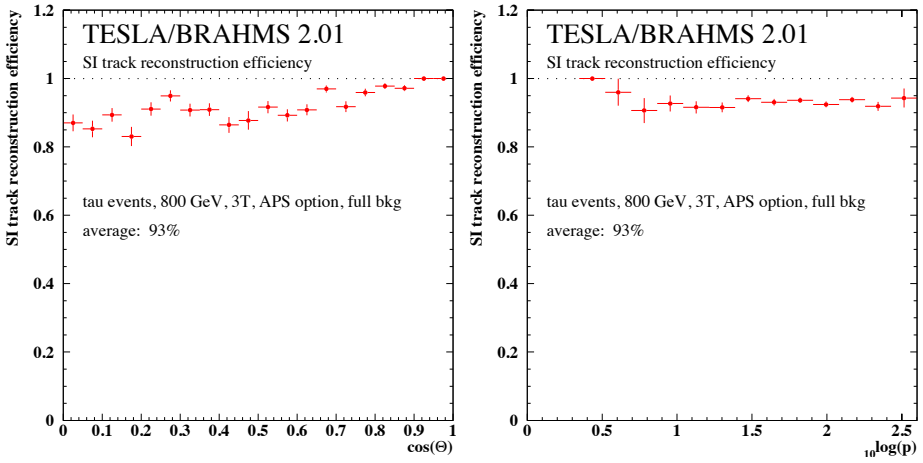

Fig. 9. Local track search efficiency in the APS variant of the central silicon detector system (APS-VTX, SIT, FTD), with full background simulation on the $\tau^+\tau^-$ reference sample, over $|\cos(\theta)|$ (left) and over the track momentum (right).

are lost (see Figure 8). Almost 10% of all track candidates are noise tracks, which is reasonable given the large background on the inner vertex detector layers. Most fake tracks are however removed in the later stages of track reconstruction, when information especially from the TPC is taken into account additionally.

The APS performance on the $\tau^+\tau^-$ sample is slightly degraded; only 93% of all tracks are found. Figure 9 shows that tracks of all momenta are equally affected, but that the efficiency loss is restricted to the barrel region, whereas the forward direction is hardly affected. The explanation for this effect has been found in a significant number of τ 3-prong decays that involve intermediate neutral resonances like K^0_S, a fraction of which decays outside the first vertex detector layer. The number of layers which are hit by the charged products

of these decays in the APS option is thus four or even less, which causes inefficiencies in the reconstruction of these tracks. Due to the redundant design of the track reconstruction detector system, full efficiency is recovered during the following global track search, where unassociated SIT and APS hits are matched to TPC track elements (see below).

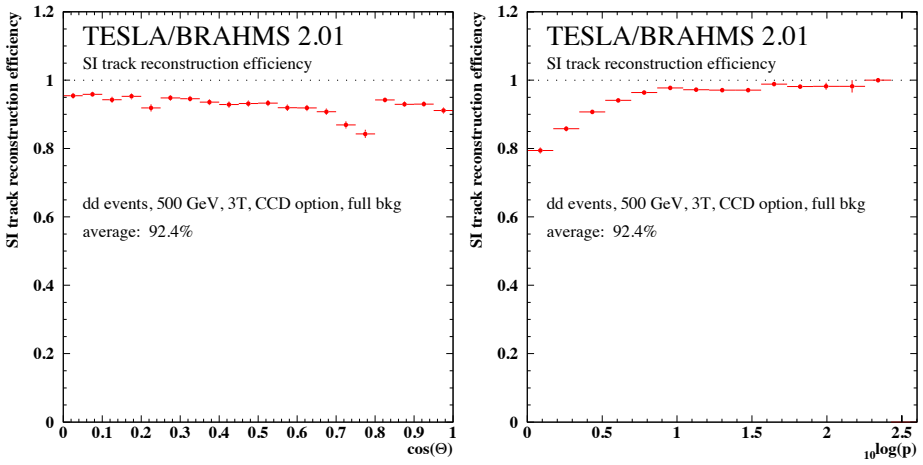

Fig. 10. Local track search efficiency in the CCD version of the central silicon detector system (CCD-VTX, SIT, FTD), with full background simulation on the $d\bar{d}$ reference sample, over $|\cos(\theta)|$ (left) and over the track momentum (right).

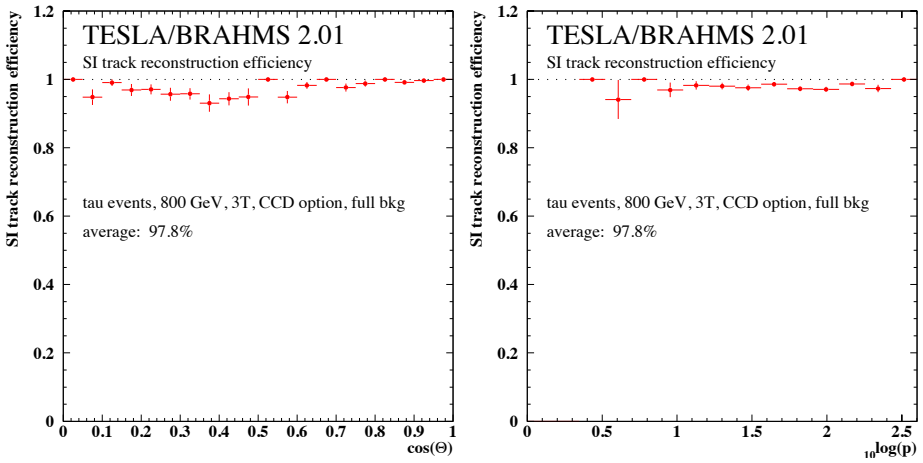

Fig. 11. Local track search efficiency in the CCD version of the central silicon detector system (CCD-VTX, SIT, FTD), with full background simulation on the $\tau^+\tau^-$ reference sample, over $|\cos(\theta)|$ (left) and over the track momentum (right).

The CCD vertex detector option is equipped with more barrel layers than the APS, which suppresses effects like the one observed for τ decay products in the APS version, but the CCD suffers from a much higher background level. With moderate background like expected for a CMOS pixel detector design of otherwise similar specifications to the CCD proposal, average reconstruction efficiencies of above 99% have been achieved. With full background simulation, the first two CCD layers are excluded from the local track search, which

negatively affects the reconstruction efficiency mainly for tracks with significant curvature, i.e. with a momentum below about 5 GeV. An efficiency of 92.4% has been found for $d\bar{d}$ events in this environment (see Figure 10), with a fraction of fake candidates of only 0.7%. The $\tau^+\tau^-$ sample contains mainly high momentum tracks which are not affected by the efficiency loss described above, and thus a reconstruction efficiency of 97.8% has been measured independent of the background level (Figure 11). 12% of all local track candidates found in the full background scenario are fakes.

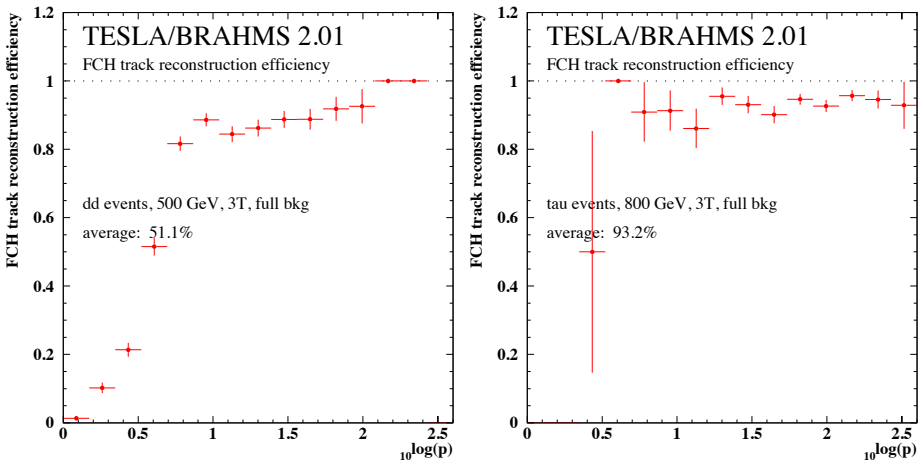

Fig. 12. Local track search efficiency in the FCH, with full background simulation, on the $d\bar{d}$ (left) and the $\tau^+\tau^-$ reference sample (right).

The third local track search takes place in the system of forward chambers (FCH) behind both TPC endcaps. As mentioned already, the large amount of material in front of the FCH restricts useful measurements in the FCH to very high-momentum tracks. Figure 12 shows that this goal has certainly been met. A reconstruction efficiency of around 90% for tracks above 10 GeV is observed. Between 7% ($d\bar{d}$) and 23% ($\tau^+\tau^-$) of all candidates are noise tracks, including tracks where the wrong drift direction has been assumed in more than 3 out of 12 layers.

4.2 Track efficiencies and fake rates in $Z \to d\bar{d}$ events at 500 GeV

It has been mentioned during the discussion of the local track search performance in the previous section, that most inefficiencies are cured during the later stages of track reconstruction, namely the global track search and ambiguity resolving. In the CCD option detector, for example, the silicon detector pattern recognition suffers slightly from the high background level. However, after merging the information delivered by all subdetectors, the global track reconstruction efficiency turns out to be 98.4%, higher than both the TPC and the silicon detector reconstruction efficiencies. The APS design, with its better reconstruction performance due to less background, achieves even 99.2%

efficiency (see Figure 13).

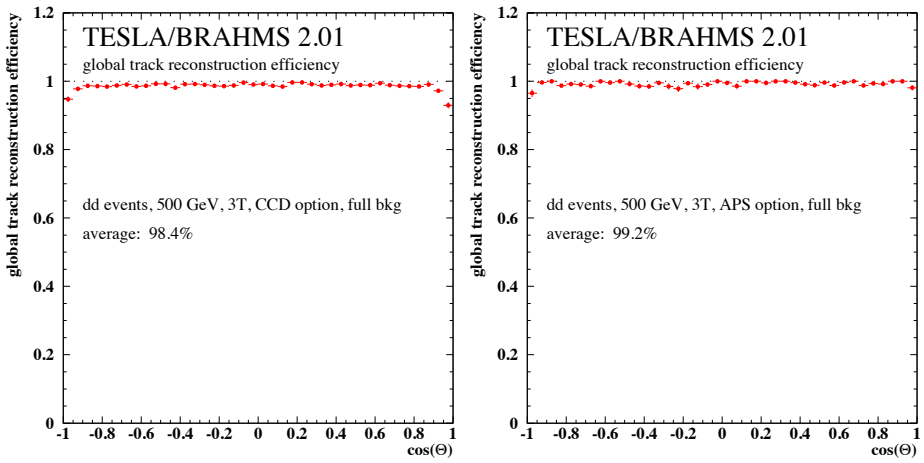

Fig. 13. Global track reconstruction efficiency over $\cos(\theta)$, with full background simulation, for the $d\bar{d}$ reference sample, CCD (left) and APS (right) option.

The fraction of fake tracks among the global track candidates is less than 1% for both vertex detector options. Roughly half of this sample consists of short track pieces dominated by noise in the silicon detectors. The remaining fake tracks are mainly short track pieces in the TPC which consist of merged hits from two or more close-by tracks. Less than 6% of the fake tracks, i.e. less than 0.06% of all track candidates, are caused by incorrect merging of correctly reconstructed local track candidates from the different subdetectors.

About 4% of all tracks are split up into at least two parts during the reconstruction. More than half of these splittings occur within the TPC; the remainder is mainly cut between the inner edge of the TPC and the silicon detectors. An explanation for the splittings within the TPC was given above; this is probably caused by distorted signals due to hit merging. The second contribution has not been investigated in detail, but could presumably be suppressed by further optimising the global track search parameters.

4.3 Track efficiencies and fake rates in $Z \to \tau^+\tau^-$ 3-prong events at 800 GeV

The extreme case of a sample of pure τ 3-prong jets pushes the demands imposed on the track reconstruction at a TESLA detector even further. As Figure 14 shows, tracks in these events are reconstructed with an overall efficiency of almost 98% for both investigated detector design variants.

The fake track fraction is significantly higher than in the $d\bar{d}$ sample, namely between 4% and 5%. The same sources as in the $d\bar{d}$ sample contribute: Short noisy track pieces in the silicon detectors and short TPC track elements with

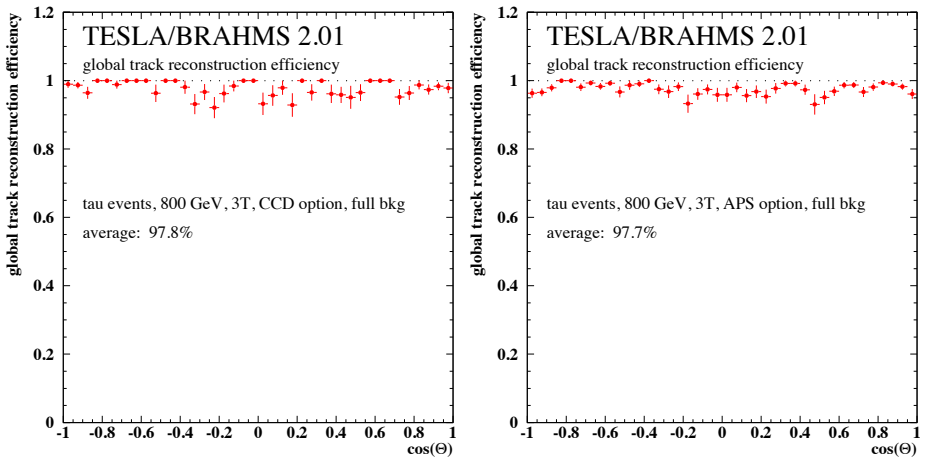

Fig. 14. Global track reconstruction efficiency over $\cos(\theta)$, with full background simulation, for the $\tau^+\tau^-$ reference sample, CCD (left) and APS (right) option.

a mixup of two or more close tracks, where this distorted piece has been separated from other, unaffected parts of the TPC tracks which were then correctly merged to their silicon counterparts. The $\tau^+\tau^-$ sample is however much more affected by a third class of fake tracks, which are correctly reconstructed silicon track elements merged to noisy TPC track parts.

The fraction of tracks that are split into at least two parts is also higher than in the case of $d\bar{d}$ events. 9% of all tracks are affected. With an increasing number of tracks that cannot be separated from nearby tracks in the inner region of the TPC, finding corresponding track pieces in TPC and silicon detectors becomes increasingly difficult. At the same time, due to more hits being lost due to merging, also the fraction of track splittings within the TPC is larger. Both effects are related, and thus it is well understandable that the relative size of their contributions to the total rate of track splittings remains the same as in the $d\bar{d}$ sample.

4.4 Hit efficiencies and fake rates for the different detector components

It has been pointed out that it is not sufficient to exploit the redundant design of the tracking detector system in that way that each track is only reconstructed in one subdetector system, while reconstruction in other systems fails frequently. All systems have to contribute information to global track candidates to make the full system meet the design criteria. In this section, it will be shown that the proposed detectors do exploit the contributions from all subsystems to an almost optimal extent. This can be investigated by looking at the association efficiency of hits in a subdetector to the track they are caused by.

The global track search and ambiguity resolving algorithms that are performed during the track reconstruction process are designed to check for subdetectors that do not yet contribute to a track candidate, and attempts are made to add the missing hits. This is especially important in the case of the CCD vertex detector, where the first two layers are not used in the initial local track search. It turns out that in $d\bar{d}$ events 94.9% and 94.3% of all hits on CCD layers 1 and 2, respectively, are correctly merged into the global track candidate. Despite the enormous background level on these layers, only 5.1% and 0.9% of all tracks pick up wrong hits on layer 1 and 2, respectively.

Differences between local track search efficiency and association efficiency are caused by two competing effects: A small fraction of hits or track elements is usually lost due to merging inefficiencies. On the other hand, additional hits are included during the global track search. In the case of good local track search performance, both numbers are expected to be about equal. For example, the APS option silicon detector system reconstructs 97.4% of all tracks traversing it in $d\bar{d}$ events correctly. 97.5% of all global track candidates include correct silicon detector information. A slightly different situation is evident in the case of the CCD track search: Whereas the local CCD track search reconstructs only 92.4% of all tracks passing the silicon detectors, in the end 96.7% of those tracks are correctly reconstructed and include silicon detector information (see Figure 15).

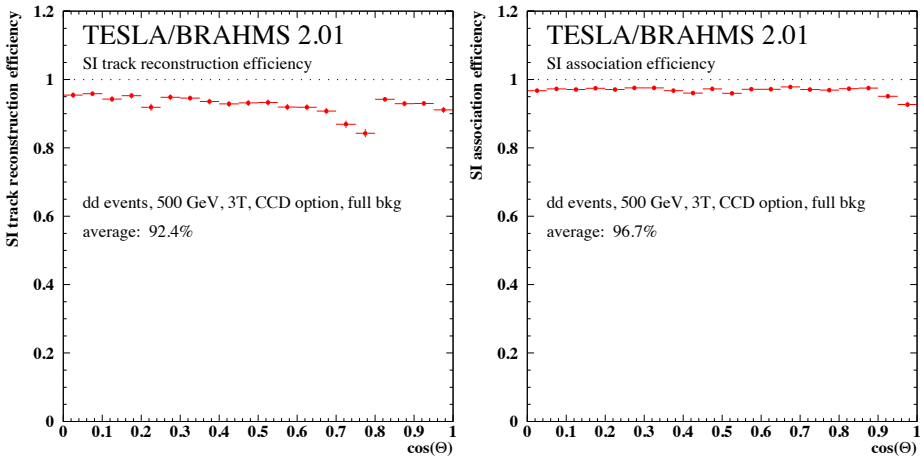

Fig. 15. Local silicon (CCD option) track reconstruction efficiency over $\cos(\theta)$, with full background simulation, for the $d\bar{d}$ reference sample (left). The right plot shows the global efficiency for the silicon detector system, or the efficiency to associate hits from the silicon detector systems correctly to the tracks that traverse this detector. The fact that the association efficiency is higher than the local track reconstruction efficiency over essentially the full angular range shows the impact of improving the local track search during the global track search and ambiguity resolving phase.

For almost all considered scenarios, the association efficiencies for silicon hits and TPC track elements are very close to the local pattern recognition efficiencies, with the exception of the two innermost CCD layers, where no local

pattern recognition is performed, as described above. The reason for these two figure of merits being close together is that the merging of the local track search result works with only small inefficiencies, and on the other hand the performance of the local track searches is good enough to leave not much room for improvement during the later reconstruction phases. The only case which is therefore to be mentioned explicitly here, in addition to the examples given above, is the inclusion of FCH track candidates into global tracks (see Figure 16). The local FCH track is not improved during the global track search, and therefore the local track reconstruction efficiency represents an upper boundary for the association efficiency; only tracks that have been found locally in the FCH can include FCH information. The association efficiency has been found to be about 7% lower than the local track reconstruction efficiency, i.e. 7% of all reconstructed FCH tracks are not successfully merged to global track candidates. This reflects the difficult situation caused by a large amount of material in the TPC endcaps between FCH and all other parts of a track. The fraction of fake associations is however only 0.6%.

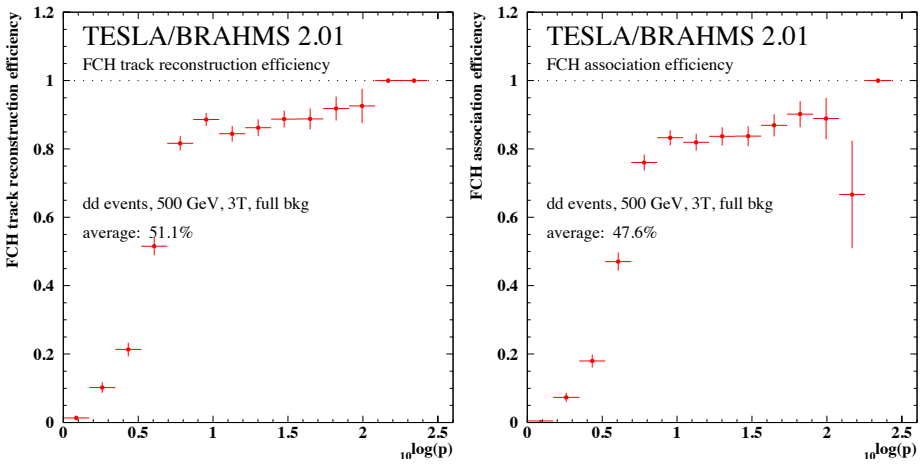

Fig. 16. Local FCH track reconstruction efficiency over track momentum, with full background simulation, for the $d\bar{d}$ reference sample (left). The right plot shows the global efficiency for the FCH, or the efficiency to associate track candidates from the FCH correctly to reconstructed global track candidates. Merging inefficiencies of about 6% are visible.

4.5 Momentum, vertex, and direction resolutions

The realistic track reconstruction package described in this note has been used to study whether the design criteria imposed on the tracking detector system can be fulfilled. A transverse momentum resolution of $\delta(\frac{1}{p_t}) \leq 5 \times 10^{-5}(\mathrm{GeV/c})^{-1}$ is required for physics analysis [2]. Figure 17 shows that this criterion can be met, and that a good momentum resolution is maintained over a large angular range.

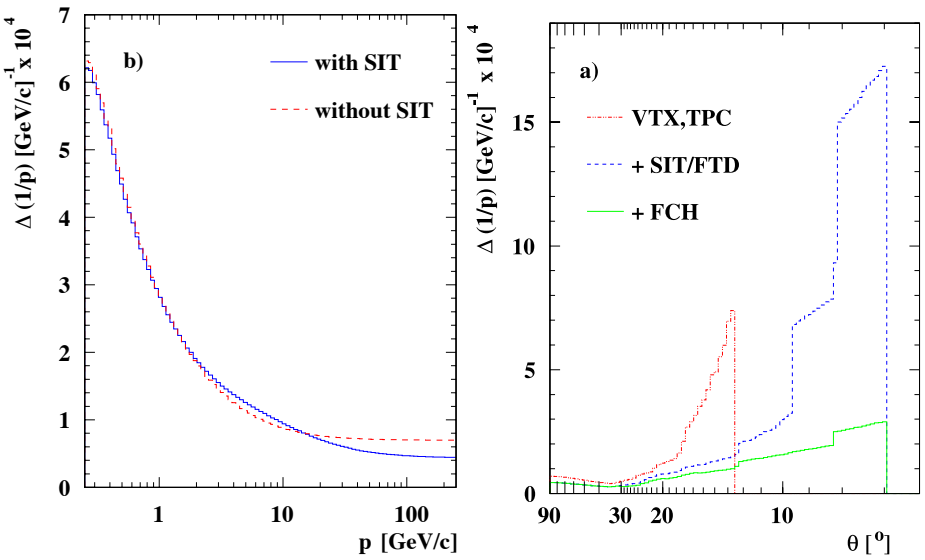

Fig. 17. Momentum resolution as a function of the momentum for tracks perpendicular to the beam axis (left). Momentum resolution for 250 GeV muons as a function of the polar angle (right). These Figures have been taken from Ref. [2].

An impact parameter resolution of $5\mu\text{m} \oplus \frac{10\mu\text{m GeV/c}}{p\sin(3/2\Theta)}$ [2] is mandatory for b and c tagging and separation with sufficient quality. The actual performance of the CCD vertex detector simulation has been measured to be $4.2\mu\text{m} \oplus \frac{4.00\mu\text{m GeV/c}}{p\sin(3/2\Theta)}$ [14] (see Figure 18).

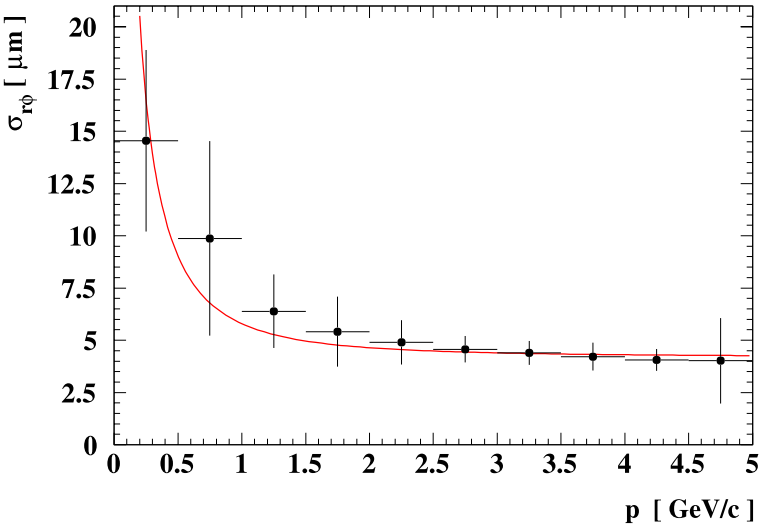

Fig. 18. Impact parameter resolution over momentum ($\theta = 90°$) as achieved with the CCD vertex detector option in the simulation framework described in this note. The fit to the distribution results to $4.2\mu\text{m} \oplus \frac{4.00\mu\text{m GeV/c}}{p\sin(3/2\Theta)}$. This figure has been taken from Ref. [14].

For angles close to the beam pipe, a major requirement is given by the desire to measure Bhabha acolinearity, which needs precise measurement of the polar angle θ. $\delta_\theta < 50\mu$rad down to $\theta \approx 7°$ for muons with momentum above 10

GeV/c has been set as aim [2]. The distribution plotted in figure 19 shows that this can be achieved.

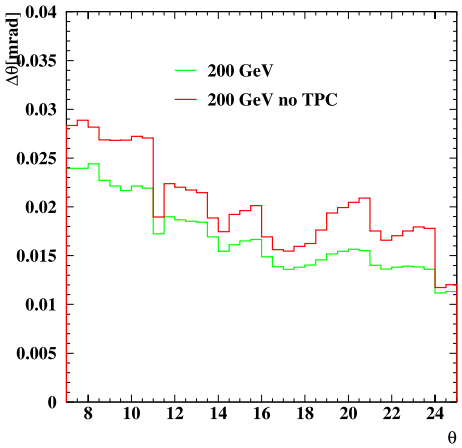

Fig. 19. Polar angle resolution for 200 GeV/c muons as a function of the polar angle. This figure has been taken from Ref. [2].

5 Conclusions

A realistic track reconstruction package has been compiled that operates on a full simulation of a detector for the TESLA linear collider, with only minor deviations from the detector design brought forward in the technical design report [2]. The performance of the detector has been evaluated with background in all detectors and pessimistic assumptions on properties of events to be reconstructed with this detector. It has been shown that, in all investigated scenarios, the detector clearly fulfills all design criteria.

Of special interest is the comparison of the performance of the APS and CCD vertex detector options. Under realistic assumptions on material, resolution, background rate, and readout technology, it has been shown that both options provide very good pattern recognition capabilities and fulfill the performance goals set by the expected physics tasks at a next generation linear collider.

Acknowledgements

We thank our collaborators within the DESY/ECFA study for the constructive and positive help in preparing this article.

References

[1] R.D. Heuer, D. Miller, F. Richard, P.M. Zerwas (Editors), *TESLA Technical Design Report, Part III: Physics at an e^+e^- Linear Collider*, DESY-2001-011, ECFA-2001-209.

[2] T. Behnke, S. Bertolucci, R.D. Heuer, R. Settles (Editors), *TESLA Technical Design Report, Part IV: A Detector for TESLA*, DESY-2001-011, ECFA-2001-209.

[3] T. Behnke, G.A. Blair et al., *BRAHMS: A Monte Carlo for a Detector at a 500/800 GeV Linear Collider*, LC-TOOL-2001-005.

[4] G. Deptuch et al., *Design and Testing of Monolithic Active Pixel Sensors for Charged Particle Tracking* , LC-DET-2001-017.

[5] M. Schumacher, *Pad Readout Geometries for a TPC with GEM Readout for the TESLA Linear Collider*, LC-DET-2001-014.

[6] M. Gruwé, *Studies of dE/dx Capabilities of a TPC for the Future Linear Collider TESLA*, LC-DET-2001-043.

[7] C.J.S. Damerell, *A CCD-based Vertex Detector for TESLA*, LC-DET-2001-023.

[8] R. Hawkings, *Vertex Detector and Flavour Tagging Studies for the TESLA Linear Collider*, LC-PHSM-2000-021.

[9] R. Frühwirth, Nucl. Instr. and Meth. **A 262** (1987) 444.

[10] P. Billoir, Nucl. Instr. and Meth. **225** (1984) 352.

[11] M. Elsing, Nucl. Instr. and Meth. **A 447** (2000) 76.

[12] D. Wicke, *A New Algorithm for Solving Tracking Ambiguities*, LC-TOOL-1999-007.

[13] H. Vogt, *Event Display for TESLA*, software available from `http://www-zeuthen.desy.de/lc_repository/dev/EVENT_DISPLAY`

[14] S.M. Xella-Hansen et al., *Flavour Tagging Studies for the TESLA Linear Collider*, LC-PHSM-2001-024.